

Quantum parameter space of dissipative directed transport

Leonardo Ermann* and Gabriel G. Carlo†

Departamento de Física, CNEA, Libertador 8250 (C1429BNP), Buenos Aires, Argentina

(Received 13 October 2014; published 26 January 2015)

Quantum manifestations of isoperiodic stable structures (QISSs) have a crucial role in the current behavior of quantum dissipative ratchets. In this context, the simple shape of the ISSs has been conjectured to be an almost exclusive feature of the classical system. This has drastic consequences for many properties of the directed currents, the most important one being that it imposes a significant reduction in their maximum values, thus affecting the attainable efficiency at the quantum level. In this work we prove this conjecture by means of comprehensive numerical explorations and statistical analysis of the quantum states. We are able to describe the *quantum parameter space* of a paradigmatic system for different values of \hbar_{eff} in great detail. Moreover, thanks to this we provide evidence on a mechanism that we call *parametric tunneling* by which the sharp classical borders of the regions in parameter space become blurred in the quantum counterpart. We expect this to be a common property of generic dissipative quantum systems.

DOI: [10.1103/PhysRevE.91.010903](https://doi.org/10.1103/PhysRevE.91.010903)

PACS number(s): 05.45.Mt, 05.60.Gg

The idea of directed transport [1] proved to be very fruitful, and has attracted a huge interest in recent years [2]. It can be very briefly defined as transport phenomena in spatial and time periodic systems which are not subject to thermal equilibrium. The current appears since all spatiotemporal symmetries leading to momentum inversion are broken [3]. Examples of ratchet models (as they are also usually referred to) have found application in many areas of research. Here we will mention just a few, such as biology [4], nanotechnology [5], granular crystals [6], and some chemical reactions as isomerization [7]. This gives an idea of how different the fields of interest could be.

At the classical level, deterministic ratchets with dissipation are generally associated with an asymmetric chaotic attractor [8]. Quantum ratchets show very rich behavior [9]. In this respect we should mention that cold atoms in optical lattices have been deeply investigated from both the theoretical and experimental points of view [10,11]. This extends also to Bose-Einstein condensates, which have been transported by means of quantum ratchet accelerators [12], where the current has no classical counterpart [13] and the energy grows ballistically [14,15]. Within this framework, a dissipative quantum ratchet interesting for cold atoms experiments has been introduced in [16]. Very recently, the parameter space of the classical counterpart of this system has been the object of a detailed study [17,18]. There it has been found that families of isoperiodic stable structures (ISSs are Lyapunov stable islands, generic in the parameter space of dissipative systems), have a very important role in the description of the currents. Subsequently, the effects of temperature have been included in the investigations leading to the determination of resistant optimal ratchet transport in its presence [19].

When looking at the quantum counterparts of these structures it has recently been found that, in general, the quantum manifestations of isoperiodic stable structures (QISSs) look like the quantum chaotic attractors at their vicinity in parameter space [20]. In other words, the simple structure of the classical

ISSs has been conjectured to be an almost exclusive property of the classical system. Just in comparatively few cases the quantum structures are similar to these classically simple objects (periodic points in the case of maps). One of the main results of this Rapid Communication consists of providing a comprehensive proof to this conjecture. For that purpose, we give a complete description of the *quantum parameter space* for two different \hbar_{eff} values. On the other hand, we show how the regions that can be associated with ISS families become interwoven at the quantum level, blurring their classically sharp borders, and thus giving rise to what we call *parametric tunneling*.

The system under investigation is a paradigmatic dissipative ratchet system given by the map [16,19,20]

$$\begin{aligned}\bar{n} &= \gamma n + k[\sin(x) + a \sin(2x + \phi)], \\ \bar{x} &= x + \tau \bar{n},\end{aligned}\tag{1}$$

where we have denoted by n the momentum variable conjugated to x , τ being the period of the map and γ the dissipation parameter. These equations describe a particle moving in one dimension [$x \in (-\infty, +\infty)$] subjected to the periodic kicked asymmetric potential

$$V(x,t) = k \left[\cos(x) + \frac{a}{2} \cos(2x + \phi) \right] \sum_{m=-\infty}^{+\infty} \delta(t - m\tau); \tag{2}$$

again τ is the kicking period, having a dissipation parametrized by $0 \leq \gamma \leq 1$. $\gamma = 0$ corresponds to the particle in the overdamped regime and $\gamma = 1$ to the conservative evolution. The directed transport appears due to broken spatial ($a \neq 0$ and $\phi \neq m\pi$) and temporal ($\gamma \neq 1$) symmetries; we take $a = 0.5$ and $\phi = \pi/2$ in this work. The classical dynamics depends only on the parameter $K = k\tau$, which can be directly noticed when introducing the rescaled momentum $p = \tau n$.

The quantum version can be obtained following a standard procedure: $x \rightarrow \hat{x}$, $n \rightarrow \hat{n} = -i(d/dx)$ ($\hbar = 1$). Since $[\hat{x}, \hat{p}] = i\tau$, the effective Planck constant is $\hbar_{\text{eff}} = \tau$. The classical limit corresponds to $\hbar_{\text{eff}} \rightarrow 0$, while $K = \hbar_{\text{eff}} k$ remains constant. Dissipation can be introduced thanks to the

*ermann@tandar.cnea.gov.ar

†carlo@tandar.cnea.gov.ar

master equation [21] for the density operator $\hat{\rho}$ of the system

$$\dot{\hat{\rho}} = -i[\hat{H}_s, \hat{\rho}] - \frac{1}{2} \sum_{\mu=1}^2 \{\hat{L}_\mu^\dagger \hat{L}_\mu, \hat{\rho}\} + \sum_{\mu=1}^2 \hat{L}_\mu \hat{\rho} \hat{L}_\mu^\dagger. \quad (3)$$

Here $\hat{H}_s = \hat{n}^2/2 + V(\hat{x}, t)$ is the system Hamiltonian, $\{, \}$ is the anticommutator, and \hat{L}_μ are the Lindblad operators given by

$$\begin{aligned} \hat{L}_1 &= g \sum_n \sqrt{n+1} |n\rangle \langle n+1|, \\ \hat{L}_2 &= g \sum_n \sqrt{n+1} |-n\rangle \langle -n-1|, \end{aligned} \quad (4)$$

with $n = 0, 1, \dots$ and $g = \sqrt{-\ln \gamma}$ (according to the Ehrenfest theorem). We have evolved 10^6 classical random initial conditions having $p \in [-\pi, \pi]$ and $x \in [0, 2\pi]$ ($\langle p_0 \rangle = 0$) in all cases, and also their quantum density operator counterpart in a Hilbert space of dimension N .

In [17–19] several classical parameter space portraits have been shown. Thanks to them three main kinds of ISSs were identified and called B_M , C_M , and D_M , where M stands for an integer or rational number and corresponds to the mean momentum of these structures in units of 2π . With the exception of $\gamma \rightarrow 1$ (i.e., near the conservative limit), ISSs organize the parameter space structure and then are essential to understand the current behavior. In previous work [20], sampling a set of relevant points in the quantum parameter space has been the only possibility, due to computational restrictions. In this Rapid Communication we report a major breakthrough in this direction, since we were able to completely extend these classical results and provide quantum parameter space portraits in the areas of interest. This can be seen in Fig. 1, where we show the quantum current J_q (we take $J_q, J_c = \langle p \rangle$, where $\langle p \rangle$ stands for either the quantum or classical average momentum, respectively) as a function of parameters k and γ . The upper panel corresponds to $\hbar_{\text{eff}} = 0.411$, while the lower one corresponds to $\hbar_{\text{eff}} = 0.137$, both having a resolution of 170×100 points. They have been obtained by using a cluster having more than 100 processors. It is noticeable how the large B_1 structure is almost the only clearly recognizable feature that resembles the classical ISSs found in parameter space. There is also a poorly defined region of positive current that can be attributed to one of the higher order B families. However, the areas associated with chaotic attractors are recognizable, especially the ones at $k \sim [3.0, 4.0]$ and $\gamma \sim [0.6, 0.8]$.

In order to investigate what happens with the other ISSs that seem not to have a quantum counterpart and also the behavior of the B_1 QISS, we explore the three highlighted regions [green (gray) squares] of Fig. 1 in more detail. In Fig. 2 we show zooms (100×100 points) taken inside these areas, the upper row corresponding to $\hbar_{\text{eff}} = 0.411$, the middle one to $\hbar_{\text{eff}} = 0.137$, and the lower row to the classical counterparts for an easier visualization of the differences between the classical and quantum results. In the left column we can appreciate how the largest of the C structures (C_{-1}) influences the B_1 region. This causes a lowering of the current inside the positive ISS region that is remarkably more pronounced in the $\hbar_{\text{eff}} = 0.137$ case than for $\hbar_{\text{eff}} = 0.411$. This indicates a kind of tunneling of one structure into the other and since this takes place

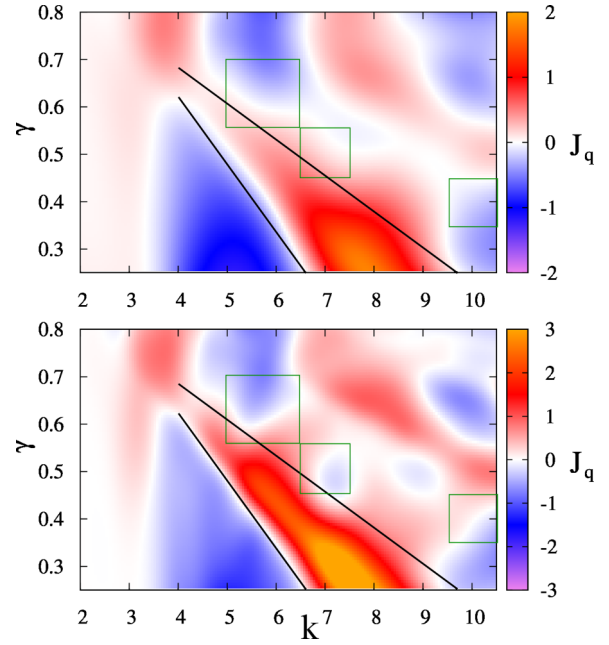


FIG. 1. (Color online) Quantum current J_q as a function of parameters k and γ in a grid of 170×100 points. The upper panel corresponds to $\hbar_{\text{eff}} = 0.411$, while the lower one corresponds to $\hbar_{\text{eff}} = 0.137$. Black lines correspond to the classical sharp borders of the B_1 structure (as in Fig. 1 of [17]). Green (gray) squares highlight the regions shown in Fig. 2.

in the parameter space, we propose it as the definition of parametric tunneling. Also, there is a positive current chaotic region different from the B_1 structure but contiguous to it, that forms a continuum with B_1 at the quantum level. The middle column shows the next zoom area that is connected with the previous one by its upper-left corner as can be seen

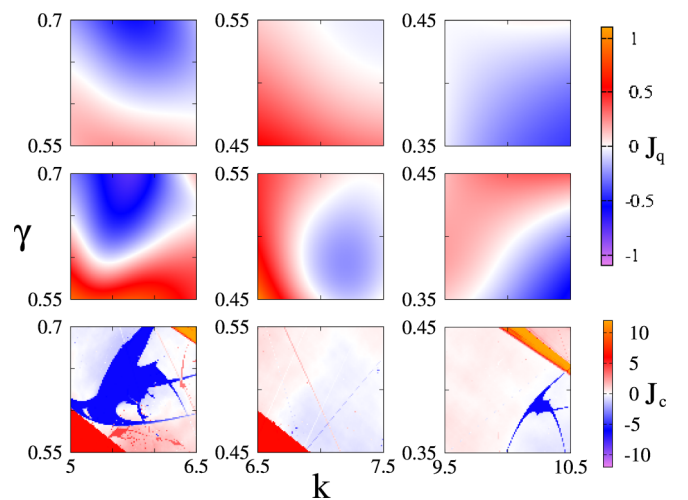


FIG. 2. (Color online) Quantum current J_q for the three different regions highlighted by means of green (gray) squares in Fig. 1. The upper panels correspond to $\hbar_{\text{eff}} = 0.411$, while the middle ones correspond to $\hbar_{\text{eff}} = 0.137$. Bottom row shows the classical counterparts (classical current J_c) for comparison purposes. All grids are of 100×100 points.

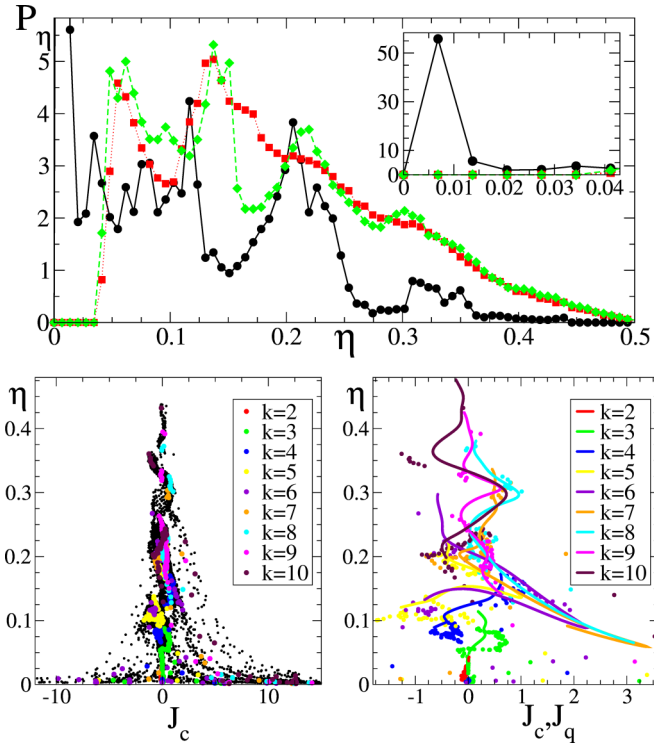


FIG. 3. (Color online) Top panel shows the participation ratio histograms P_η as a function of η . Statistics corresponds to all the cases shown in Fig. 1. Classical P_η is represented with black circles (solid line), and quantum P_η for $\hbar_{\text{eff}} = 0.411$ and $\hbar_{\text{eff}} = 0.137$ with red (dark gray) squares (dotted line) and green (light gray) diamonds (dashed line), respectively. Inset shows the same histograms in the $\eta \in [0 : 0.05]$ range. Bottom left panel: Black circles represent η as a function of J_c , with integer values of k in different shades of gray (colors). Bottom right panel: Comparison of classical (circles) and quantum (lines) η as a function of J_q, J_c for $\hbar_{\text{eff}} = 0.137$ with integer values of $k = 2, \dots, 10$ and 100 values of $\gamma \in [0.2, 0.8]$.

in Fig. 1. It shares the mentioned positive current region and also has a negative current chaotic zone. This latter also has an influence on the B_1 structure, a phenomenon that is clearly more marked for the lower $\hbar_{\text{eff}} = 0.137$ case and that can be appreciated with the help of the central panel in Fig. 2. Finally, the right column shows an isolated area corresponding to one part of the D_{-1} structure which seems to faintly manifest itself through negative currents but whose shape makes it difficult to precisely relate it to its classical counterpart. In fact it seems to be merged with the negative current chaotic region embedding it.

In order to systematically prove that simple (pointlike) structures are exceptional at the quantum level, we have analyzed the shape of the limiting quantum momentum distributions (obtained after 50 time steps) by means of the participation ratio $\eta = [\sum_i P(p_i)^2]^{-1}/N$. This measure is a good indicator of the fraction of basis elements that effectively expands the quantum state. For comparative purposes we have also calculated the corresponding classical η by taking a discretized p distribution (after 10 000 time steps), having a number of bins given by the Hilbert space dimension of the lower \hbar_{eff} case (this being $N = 3^6$). It is clear that a

finer coarse-graining would slightly change the classical η distributions but this will not affect their main properties. This is because the distance among points of the ISSs is almost always greater than the chosen bin size. We have calculated the histograms P_η vs η , and we have also studied how η behaves as a function of the current J_q, J_c . Results are shown in Fig. 3, where the upper panel corresponds to the histograms (normalized to 1) for all the cases shown in Fig. 1. The classical P_η values (black circles and solid line) have a peak at extremely low η , which can be seen in the inset. The quantum P_η for $\hbar_{\text{eff}} = 0.411$ [red (dark gray) squares and dotted line] and $\hbar_{\text{eff}} = 0.137$ [green (light gray) diamonds and dashed line] have larger values at the tail of the distributions. These are the most important properties and they are enough to prove our conjecture. Moreover, with the exception of the peak around $\eta = 0.2$ the classical distribution falls below 0.01 very quickly, while the quantum ones acquire finite values after $\eta \sim 0.03$. On the other hand, the quantum distribution for $\hbar_{\text{eff}} = 0.137$ starts to follow the shape of the classical one for higher η but it is almost unchanged with respect to $\hbar_{\text{eff}} = 0.411$ for the lowest values. In the bottom left panel in Fig. 3 we can see that the maximum J_c correspond to the lowest η , and when superimposed to the quantum values (see Fig. 3, bottom right panel) they roughly match them for some of the lowest J_q, J_c . In general the classical η are extremely discontinuous, a signature of the classical sharp borders of the different regions in parameter space, while the quantum ones behave smoothly, also reflecting the appearance of the corresponding parameter space. It is worth mentioning that the maximum of J_q is attained for one of the lowest η values and that can be associated to the “core” of the B_1 region (around $k = 7.5$ and

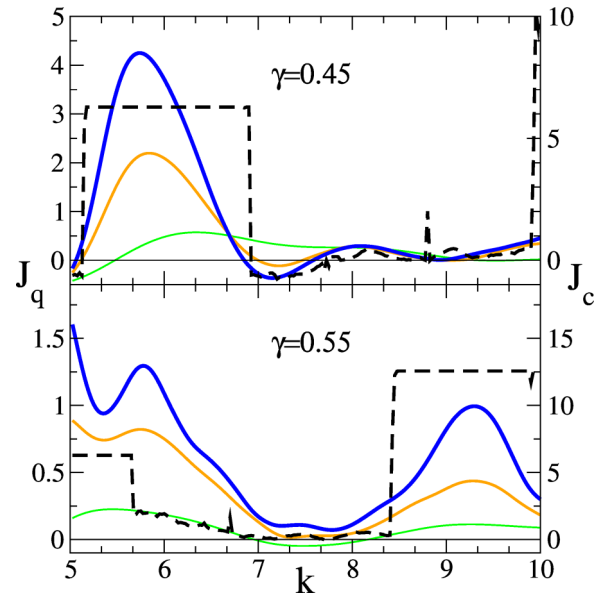


FIG. 4. (Color online) Quantum and classical current J_q and J_c as a function of parameter k for $\gamma = 0.45$ (top panel), and $\gamma = 0.55$ (bottom panel). Quantum currents are represented with solid green (light gray) lines for $\hbar_{\text{eff}} = 0.411$, orange (gray) lines for $\hbar_{\text{eff}} = 0.137$, and blue (dark gray) lines for $\hbar_{\text{eff}} = 0.068$. Their corresponding scales are shown on the left side. Classical currents are illustrated with dashed black lines with their corresponding scales on the right.

$\gamma = 0.3$). The few lower quantum η values have also much lower J_q and belong to the lowest k region.

Finally, we have selected transversal cuts of Fig. 1 for two different γ values, these being 0.45 and 0.55. This shows that the classical features are very slowly approached by the quantum distributions and also how different parameter space neighboring regions influence each other. The results are shown in Fig. 4 (upper and bottom panels, respectively), where it is important to notice that the classical current scale (on the right side) is much larger than the quantum one (on the left side). It is clearly visible that the sharp borders corresponding to the classical regions cannot be reproduced by the quantum counterparts, even though the current significantly grows as \hbar_{eff} drops from 0.411 to 0.068 for the B QISSs. Moreover we see how negative J_q, J_c values, typical of the chaotic region near B_1 that is highlighted in the middle panels of Fig. 2, also can be found inside a small portion of the B_1 area near its border (see Fig. 4, upper panel). The influence suffered from the C_{-1} structure near B_1 can be appreciated as a clear drop in J_q values inside the region corresponding to this structure (see Fig. 4, bottom panel). Again, it is remarkable that this phenomenon is more pronounced for the lowest $\hbar_{\text{eff}} = 0.068$ value.

To summarize, we have performed a comprehensive exploration of the quantum parameter space of a paradigmatic system in the directed transport, open systems, and quantum chaos literature, i.e., the dissipative quantum kicked rotator with a biharmonic kick. As a result we were able to develop a complete picture of the *quantum parameter space* for this kind of systems. Thanks to statistically exploring the limiting distributions through the participation ratios η , we have systematically proved that the simple structure of the classical ISSs is exceptional at the quantum level. This is of huge relevance for the properties of quantum directed currents, mainly limiting their maximum values and as such, reducing the efficiency. Moreover, we have found a remarkable feature of QISSs, this being the influence that they suffer among each other that blurs their classically sharp borders, a phenomenon we have called *parametric tunneling*. In the future, we will try to identify the details behind this mechanism and also its consequences at the current level. Also, we plan to consider a nonzero temperature in order to test how robust is the obtained quantum parameter space picture.

Financial support from CONICET is gratefully acknowledged.

-
- [1] R. P. Feynman, *Lectures on Physics* (Addison-Wesley, Reading, MA, 1963), Vol. 1.
- [2] P. Reimann, Brownian motors: Noisy transport far from equilibrium, *Phys. Rep.* **361**, 57 (2002); S. Kohler, J. Lehmann, and P. Hänggi, Driven quantum transport on the nanoscale, *ibid.* **406**, 379 (2005); S. Denisov, S. Flach, and P. Hänggi, Tunable transport with broken space-time symmetries, *ibid.* **538**, 77 (2014).
- [3] S. Flach, O. Yevtushenko, and Y. Zolotaryuk, Directed current due to broken time-space symmetry, *Phys. Rev. Lett.* **84**, 2358 (2000).
- [4] G. Mahmud *et al.*, Directing cell motions on micropatterned ratchets, *Nat. Phys.* **5**, 606 (2009); G. Lambert, D. Liao, and R. H. Austin, Collective escape of chemotactic swimmers through microscopic ratchets, *Phys. Rev. Lett.* **104**, 168102 (2010); S. Cocco, J. F. Marko, and R. Monasson, Stochastic ratchet mechanisms for replacement of proteins bound to DNA, *ibid.* **112**, 238101 (2014).
- [5] R. D. Astumian, Thermodynamics and kinetics of a brownian motor, *Science* **276**, 917 (1997); D. Reguera, A. Luque, P. S. Burada, G. Schmid, J. M. Rubí, and P. Hänggi, Entropic splitter for particle separation, *Phys. Rev. Lett.* **108**, 020604 (2012).
- [6] V. Berardi, J. Lydon, P. G. Kevrekidis, C. Daraio, and R. Carretero-González, Directed ratchet transport in granular chains, *Phys. Rev. E* **88**, 052202 (2013).
- [7] G. G. Carlo, L. Ermann, F. Borondo, and R. M. Benito, Environmental stability of quantum chaotic ratchets, *Phys. Rev. E* **83**, 011103 (2011); L. S. Brizhik, A. A. Eremko, B. M. A. G. Piette, and W. J. Zakrzewski, Thermal enhancement and stochastic resonance of polaron ratchets, *ibid.* **89**, 062905 (2014).
- [8] J. L. Mateos, Chaotic transport and current reversal in deterministic ratchets, *Phys. Rev. Lett.* **84**, 258 (2000).
- [9] P. Reimann, M. Grifoni, and P. Hänggi, Quantum ratchets, *Phys. Rev. Lett.* **79**, 10 (1997); L. Ermann, G. G. Carlo, and M. Saraceno, Transport phenomena in the asymmetric quantum multibaker map, *Phys. Rev. E* **77**, 011126 (2008); Behavior of the current in the asymmetric quantum multibaker map, **79**, 056201 (2009).
- [10] T. Salger, S. Kling, T. Hecking, C. Geckeler, L. Morales-Molina, and M. Weitz, Directed transport of atoms in a hamiltonian quantum ratchet, *Science* **326**, 1241 (2009).
- [11] T. S. Monteiro, P. A. Dando, N. A. C. Hutchings, and M. R. Isherwood, Proposal for a chaotic ratchet using cold atoms in optical lattices, *Phys. Rev. Lett.* **89**, 194102 (2002); G. G. Carlo, G. Benenti, G. Casati, S. Wimberger, O. Morsch, R. Mannella, and E. Arimondo, Chaotic ratchet dynamics with cold atoms in a pair of pulsed optical lattices, *Phys. Rev. A* **74**, 033617 (2006).
- [12] M. Sadgrove, M. Horikoshi, T. Sekimura, and K. Nakagawa, Rectified momentum transport for a kicked Bose-Einstein condensate, *Phys. Rev. Lett.* **99**, 043002 (2007); I. Dana, V. Ramareddy, I. Talukdar, and G. S. Summy, Experimental realization of quantum-resonance ratchets at arbitrary quasimomenta, *ibid.* **100**, 024103 (2008); D. H. White, S. K. Ruddell, and M. D. Hoogerland, Experimental realization of a quantum ratchet through phase modulation, *Phys. Rev. A* **88**, 063603 (2013).
- [13] E. Lundh and M. Wallin, Ratchet effect for cold atoms in an optical lattice, *Phys. Rev. Lett.* **94**, 110603 (2005); D. Poletti, G. G. Carlo, and B. Li, Current behavior of a quantum Hamiltonian ratchet in resonance, *Phys. Rev. E* **75**, 011102 (2007).
- [14] A. Kenfack, J. Gong, and A. K. Pattanayak, Controlling the ratchet effect for cold atoms, *Phys. Rev. Lett.* **100**, 044104 (2008); J. Wang and J. Gong, Quantum ratchet accelerator

- without a bichromatic lattice potential, *Phys. Rev. E* **78**, 036219 (2008).
- [15] M. Sadgrove, M. Horikoshi, T. Sekimura, and K. Nakagawa, Coherent control of ballistic energy growth for a kicked Bose-Einstein condensate, *Eur. Phys. J. D* **45**, 229 (2007).
- [16] G. G. Carlo, G. Benenti, G. Casati, and D. L. Shepelyansky, Quantum ratchets in dissipative chaotic systems, *Phys. Rev. Lett.* **94**, 164101 (2005).
- [17] A. Celestino, C. Manchein, H. A. Albuquerque, and M. W. Beims, Ratchet transport and periodic structures in parameter space, *Phys. Rev. Lett.* **106**, 234101 (2011).
- [18] A. Celestino, C. Manchein, H. A. Albuquerque, and M. W. Beims, Stable structures in parameter space and optimal ratchet transport, *Commun. Nonlinear Sci. Numer. Simulat.* **19**, 139 (2014).
- [19] C. Manchein, A. Celestino, and M. W. Beims, Temperature resistant optimal ratchet transport, *Phys. Rev. Lett.* **110**, 114102 (2013).
- [20] G. G. Carlo, Quantum isoperiodic stable structures and directed transport, *Phys. Rev. Lett.* **108**, 210605 (2012).
- [21] G. Lindblad, On the generators of quantum dynamical semi-groups, *Commun. Math. Phys.* **48**, 119 (1976).